

# The JWST/NIRSpec Exoplanet Exposure Time Calculator

Louise Dyregaard Nielsen<sup>a</sup>, Pierre Ferruit<sup>a</sup>, Giovanna Giardino<sup>a</sup>, Stephan Birkmann<sup>b</sup>, Antonio García Muñoz<sup>c</sup>, Jeff Valenti<sup>d</sup>, Kate Isaak<sup>a</sup>, Caterina Alves de Oliveira<sup>b</sup>, Torsten Böker<sup>b</sup>, Nora Lützgendorf<sup>b</sup>, Timothy Rawle<sup>b</sup>, and Marco Sirianni<sup>b</sup>

<sup>a</sup>European Space Agency / ESTEC, Noordwijk, The Netherlands

<sup>b</sup>European Space Agency / STScI, Maryland, The United States

<sup>c</sup>Technische Universität Berlin, Berlin, Germany

<sup>d</sup>STScI, Maryland, The United States

## ABSTRACT

The James Webb Space Telescope (JWST), with its unprecedented sensitivity, will provide a unique set of tools for the study of transiting exoplanets and their atmospheres. The Near Infrared Spectrograph (NIRSpec) is one of four scientific instruments on JWST and offers a high-contrast aperture-spectroscopy mode developed specifically for exoplanet observations.

Here we present the NIRSpec Exoplanet Exposure Time Calculator (NEETC) software, an exposure time calculator optimized to evaluate the signal-to-noise ratio and simulate spectra for observations of transiting exoplanets. The NEETC is being developed to help the NIRSpec instrument team, and ultimately future JWST users, to fully investigate NIRSpec's observation modes and the feasibility of exoplanet observations. We give examples of how the NEETC can be used to prepare observations, and present results highlighting the capabilities and limitations of NIRSpec.

**Keywords:** Exoplanets, James Webb Space Telescope, JWST, NIRSpec, Transit spectroscopy

## 1. INTRODUCTION

The diagnostic power of transit and phase-curve spectroscopy for the study of atmospheric properties of transiting exoplanets has been demonstrated for hot Jupiters, warm Neptunes and warm sub-Neptunes with the Hubble Space Telescope (HST; see e.g. [1]). The James Webb Space Telescope [JWST; 2] will provide the sensitivity, wavelength coverage and spectral resolution needed to investigate these objects in more detail and target temperate (super)-Earths.

The Near Infrared Spectrograph [NIRSpec; 3] is one of four instruments on-board JWST and will be the main workhorse for near infrared spectroscopy. It operates in the wavelength range 0.6-5.3  $\mu\text{m}$ , which provides a small wavelength overlap with the JWST Mid-Infrared Instrument [MIRI; 4], making it easier to combine NIRSpec and MIRI spectra. NIRSpec is capable of low ( $R \sim 100$ ), medium ( $R \sim 1000$ ) and high ( $R \sim 2700$ ) spectral-resolution spectroscopy in three different modes: multi-object, integral-field and high-contrast long-slit. Spectroscopy of transiting exoplanets is enabled by a square 1.6"  $\times$  1.6" aperture (named SLIT/A1600) designed to minimize the susceptibility of observations to slit losses and their variations.

Exposure time calculators (ETCs) are crucial tools for observers to understand the capabilities of an instrument and its modes by answering questions such as: what signal-to-noise ratio (SNR) will a given observation achieve? How long must an object be observed to achieve a given SNR? As part of the development of NIRSpec, the NIRSpec instrument team has developed a suite of ETC-like tools to estimate the sensitivity of the instrument (see e.g. the sensitivity curves in [5]). These tools have however been designed primarily for observations of faint objects, i.e. for observing strategies and noise regimes very different from those valid for observations of transiting exoplanets. We have therefore embarked into the development of the NIRSpec Exoplanet Exposure Time Calculator (NEETC\*), which is optimized to deal with observations of transiting exoplanets using the SLIT/A1600 aperture. In this paper we will describe the fundamentals of exoplanet observations with NIRSpec and how the NEETC will help users prepare these observations.

---

Author contact: louise.nielsen@esa.int

\*Pronounced 'nee-T-C'

## 2. OBSERVING TRANSITING EXOPLANETS WITH JWST/NIRSPEC

The basics of exoplanet transit observations are illustrated in Fig. 1. The sketch shows how the planet and its atmosphere block the starlight during transit and how during occultation, a smaller dip will appear in the light curve due to the complete loss of reflected starlight and thermal emission from the planet. The amount of light reflected and emitted by the planet changes with the phase angle as the planet orbits its host star.

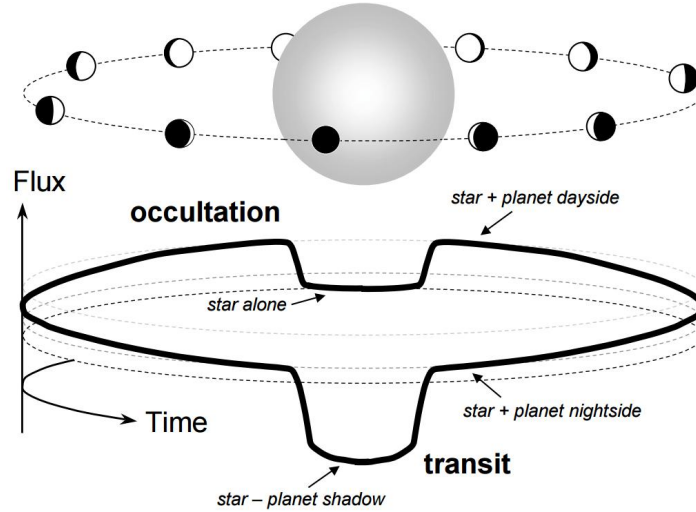


Figure 1. Schematic representation of planet transit (primary eclipse) and occultation (secondary eclipse). In this work we approximate the planet nightside to be completely black, and therefore not contributing to the total signal. Reflection and thermal emission from the planet dayside scale slightly differently with the phase angle, and are maximal right before and after the occultation. Figure from [6].

During a transit or an occultation, the planetary signal can be isolated by carrying out observations both in and out of transit/occultation. Throughout this paper we use the classic strategy of spending twice the transit duration doing baseline observations (i.e. out of transit/occultation). The transit depth is given by

$$d_T = \frac{F_{out} - F_T}{F_{out}} = \left( \frac{r_{planet} + h_{eq}(\lambda)}{r_{star}} \right)^2, \quad (1)$$

where  $F_T$  and  $F_{out}$  are the measured flux in and out of transit.  $r_{star}$  and  $r_{planet}$  are the radii of the host star and planet, respectively, and  $h_{eq}$  is the wavelength-dependent equivalent height of the planetary atmosphere. It is clear from the right hand side of Eq. 1 that big planets around small host stars are the easiest to detect and observe. In the case of occultation the measured quantity is the contrast between the brightness of the the planet and its host star:

$$C = \frac{F_{out} - F_s}{F_s}, \quad (2)$$

where  $F_s$  is the star flux (as measured during occultation).

The transit depth and brightness contrast are usually in the range of 10-100 parts per million (ppm). In order to extract meaningful information from these observations, very high SNR-data is required. The SNR of these observations scales roughly as the square root of the number of accumulated electrons, and it is therefore advantageous (in terms of SNR) to collect as many photons as possible from the host star. So we are expecting planets orbiting bright host stars to be preferred targets for exoplanet transit spectroscopy.

## 2.1 NIRSpec Detector Setup and Instrument Configurations for Transiting Exoplanets

As a consequence of the bright nature of the preferred exoplanet host stars, a specific detector setup for bright targets has recently been added for NIRSpec. It uses an electronic gain of  $2 \text{ e}^-/\text{ADU}$  to take advantage of the physical full well, instead of being limited by the 16-bit ADC, as it is the case for the baseline NIRSpec detector setup. In the NEETC and throughout this paper, a maximum number of accumulated photo-electrons of  $77 \text{ ke}^-/\text{ADU}$  is used. This corresponds to a conservative (low) estimate of the dynamical range of the instrument, which is given by the effective saturation limit minus the initial bias zero point.

The up-the-ramp readout scheme used by NIRSpec detectors, called MULTIACCUM[7], is similar to the one used by HST/NICMOS. Each signal integration will start with a reset followed by a user-defined number of non-destructive frame readouts, as illustrated in Fig. 2. An exposure consists of a series of consecutive integrations. Multiple frames can be combined on-board into groups. For exoplanet observations, each group will be made up of one frame, therefore hereafter we will only refer to number of groups per integration. In most cases it will be preferable to use at least two groups per integration (reset-read-read-...). For very bright sources however, it is possible to perform integrations with a single group (reset-read), significantly improving the actual detector duty cycle.

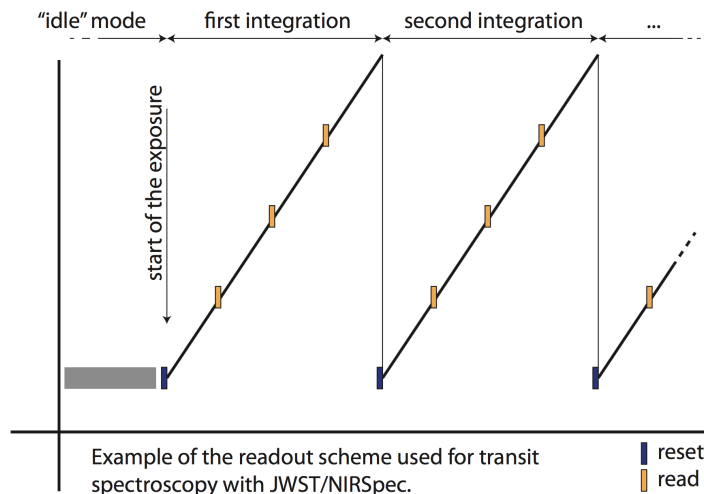


Figure 2. Illustration of the specific MULTIACCUM readout scheme used by NIRSpec when observing transiting exoplanets. In this example an individual integration consists of a reset followed by 3 groups each containing one frame. The exposure contains multiple integrations. The detector duty cycle is 75% as one fourth of each integration is used to reset the detector. Figure from [8].

To further accommodate bright target observations, we take advantage of the fact that the spectrum from SLIT/A1600 covers only a small fraction of the detectors and hence the source can be acquired from a smaller detector area, so called subarray, or detector WINDOW mode. The subarray sizes sets the readout time of the detector, and thus the minimum exposure time.

Table 1 summarizes the 9 instrument spectral configurations, including the default subarrays, supported by NIRSpec for exoplanet observations. The low-resolution mode (PRISM) allows the full wavelength range to be covered in a single exposure. The high- and medium-resolution configurations (gratings) need at least four exposures to achieve complete spectral coverage. Spectra obtained with any of the four high-resolution configurations will present wavelength gaps, due to the spacing between the two detectors in the NIRSpec focal plane. The chip gaps corresponds to up to  $0.10 \mu\text{m}$  in the spectra.

The magnitude limits listed in Tab. 1 present a worst case scenario in terms of dynamical range, where the peak of the stellar PSF is centered on a detector pixel and the shape of the spectral energy distribution (SED) results in a non-favorable normalization in the J-band. Figure 3 shows how the bright-object limit heavily depend on the spectral type of the host star.

Table 1. Overview of the key properties of the spectral configurations available in the SLIT/A1600 mode for transit spectroscopy. The magnitude limits have been estimated using gain = 2 e<sup>-</sup>/ADU and one frame per group. These values should only be used as a guideline and are still susceptible to change.

Mode	Configuration disperser / filter	Wavelength range [μm]	Resolution range	Subarray default [px]	J-mag limit (worst case)
Low	PRISM/CLEAR	0.60 - 5.30	30 - 300	512x32	9.83
Medium	F070LP/G140M	0.70 - 1.20	500 - 850	2048x32	7.75
	F100LP/G140M	1.00 - 1.80	700 - 1300		7.76
	F170LP/G235M	1.70 - 3.10	700 - 1300		7.44
	F290LP/G395M	2.90 - 5.20	700 - 1300		7.01
High	F070LP/G140H	0.82 - 1.20	1300 - 2300	2048x32	6.63
	F100LP/G140H	1.00 - 1.80	1900 - 3600		6.64
	F170LP/G235H	1.70 - 3.06	1900 - 3600		6.34
	F290LP/G395H	2.90 - 5.17	1900 - 3600		5.84

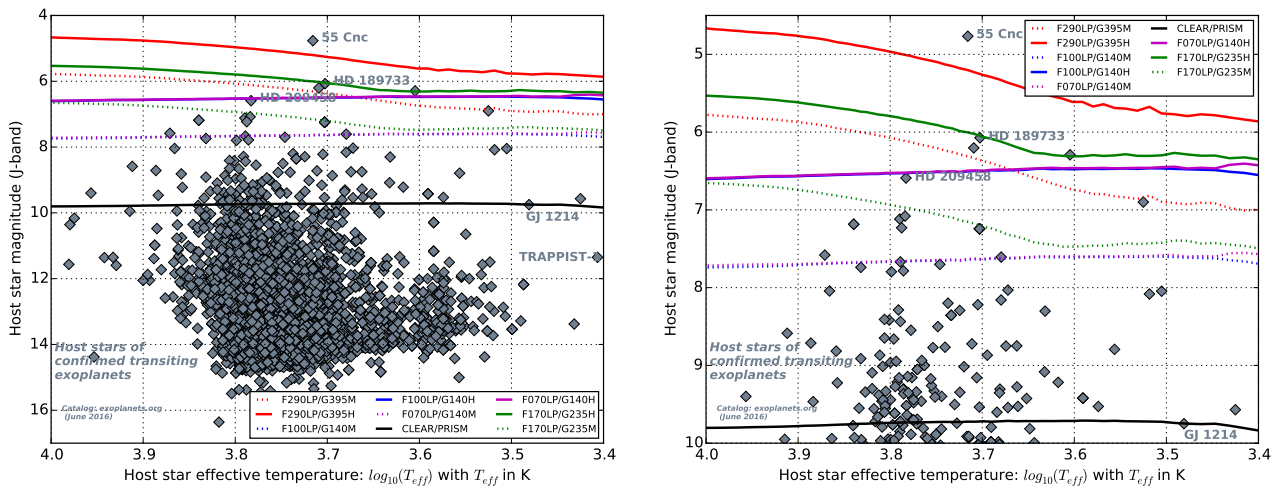


Figure 3. Estimated limiting J-band magnitude for all 9 instrument configurations supported by JWST/NIRSpec plotted as a function of the host-star effective temperature. These values are the current estimates and are still susceptible to change as our knowledge of the instrument improves. Stars with known transiting planets have been plotted as gray diamonds along with labels on a few the well-known objects. The panel on the right shows a cut-out of the left panel, concentrating on the limiting magnitudes from 10 to 4. Figure created with the NEETC.

### 3. THE NIRSPEC EXOPLANET EXPOSURE TIME CALCULATOR – NEETC

The NEETC is being developed at the European Space Agency by the NIRSpec instrument team. It is designed to model NIRSpec observations of transiting exoplanets around bright stars, using the instrument setups described in Sec 2.1. As NIRSpec offers a suite of 9 spectral configurations, it can be difficult for future observers to determine which ones are the best suited for a given observation. Furthermore, as exoplanet transmission spectroscopy is very time consuming, (see e.g. [9]), preference will likely be given to carefully selected targets. The NEETC is designed to provide the necessary tools for in depth preparatory studies of NIRSpec target candidates, including an easy comparison of the results obtained with different spectral configurations.

Both stellar and planetary components of the spectrum can be given as an input to the NEETC, along with the observation type (transit, occultation or full phase curve). The output consists of simulated spectra with representative noise-floor levels that allows the users to reliably assess the quality of the observation. The user

can also optimize the observation by calculating and comparing SNRs for multiple instrument configurations and readout setups. The number of groups per integration, which will give the best duty cycle without saturating the detector, is also computed. We call this the *optimal number of groups* in the frame work of the NEETC.

The NEETC uses photon-conversion-efficiency and dispersion curves for all 9 instrument configurations, to calculate the signal detected by NIRSpec. As mentioned in Sec. 2 a worst-case scenario is used when checking for saturation, assuming that the peak of the PSF of the target always falls at the center of a pixel, as opposed to in the corner where 4 adjacent pixels meet (yielding a maximum number of accumulated electrons per pixel typically 20-30% lower). The PSF-core size varies throughout the wavelength range from 0.5 to 1.5 physical detector pixels.

*Effective number of groups* are used to calculate the signal and SNR. This is the number of groups per integration before saturation occurs for each pixel. For example, for an exposure consisting of four groups per integration, if part of the spectrum is saturated after three groups, the SNR in these pixels will be calculated based on three groups only. This will lead to a lower efficiency (duty cycle) in this part of the spectrum, as the fourth group will be saturated and unusable.

### 3.1 Noise Model

A major challenge faced when trying to describe observations targeting SNR of several tens of thousands is that the contribution of residuals to the correction of systematic effects is often a major limiting factor. Understanding which systematics will impact NIRSpec observations and what their correction residuals will look like is extremely difficult and will likely only be possible once we have acquired in-orbit data. As a starting point, We have decided to adopt a noise model that allows us to define a so-called noise floor, corresponding to the ideal case where the contribution of systematics is absent.

Observations with current space-based facilities achieve noise levels within 20 – 30% of the photon-noise level and if we assume that JWST/NIRSpec observations will achieve the same level of performances, the NEETC results can be easily scaled. The noise model for the detectors used in the NEETC is based on a drastic simplification of the generic model described in [7]. In this model, the noise floor is calculated including the effects of readout noise, photon noise from the source and dark current shot noise. The equations listed in [7] reflect an up-the-ramp fitting optimized for faint sources, aiming to damp the contribution of the readout noise to the noise floor. For observations limited by the source photon noise (photon noise regime), which is the case for exoplanets, the best performance is achieved by ignoring the intermediate readouts and by using just the first and last group of the integration. This gives the very simple relation:

$$\sigma_{last-first}^2 = 2\sigma_{read}^2 + t_g(n_g - 1)f, \quad (3)$$

using  $t_{int} = t_g(n_g - 1)$ . For the reset-read-reset option, one must use the zero point to find the count rate. This scheme improves the duty cycle as the zero level is 'added' to the effective number of groups. The zero level noise is however not dominated by the readout noise, but by the so-called kTC noise. The total noise is in this case:

$$\sigma_{last-zero}^2 = \sigma_{read}^2 + \sigma_{kTC}^2 + t_g n_g f. \quad (4)$$

The NEETC uses  $\sigma_{kTC} = 60 \text{ e}^-$  (very conservative value) and  $\sigma_{read} = 18 \text{ e}^-$ .

### 3.2 Design

Figure 4 shows a flow chart representation of the NEETC architecture. It consists of the Core Computation model which computes effective number of groups, optimal number of groups, signal and SNR *per integration*. The user can input the stellar SED, instrument configuration and optionally number of groups per integration.

A number of additional (Post-)modules compute the signal and SNR achieved over a certain amount of time. For transit and occultation, it is assumed that twice the transit/occultation time is used on the baseline observation. The results can also be binned to a uniform spectral sampling ( $\Delta\lambda$ ), to facilitate the comparison of different observation modes.

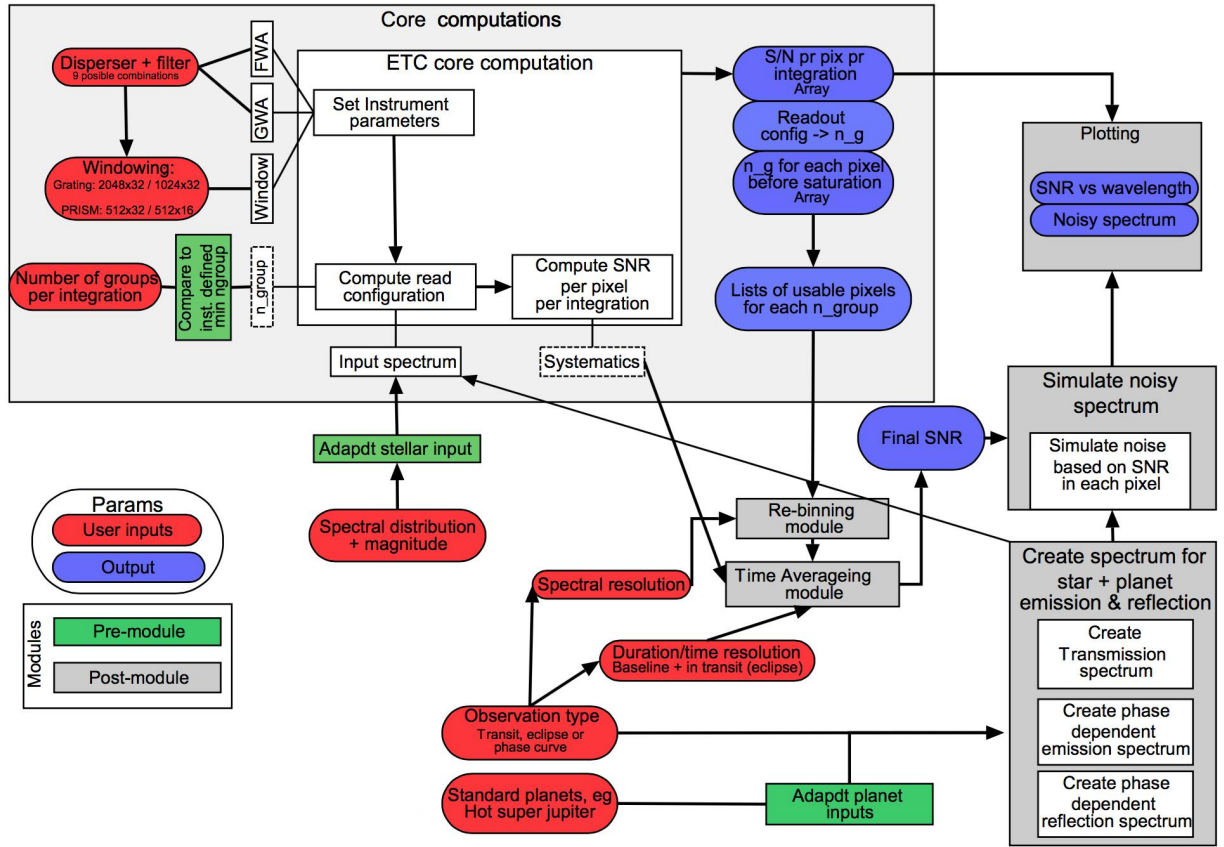


Figure 4. Flow chart representation of the main NEETC modules.

Currently, the input planetary signal can be selected from a number of synthetic spectra [10]. The contribution from the planet includes thermal emission, reflection of starlight and transmission during transit. The first two components scale differently with the phase angle as the planet orbits around its parent star. Transmission and reflection are both given as contrast to the stellar brightness, whereas thermal emission is internally implemented as an absolute brightness, which is subsequently normalized to the target distance. The NEETC combines reflection, thermal emission and transmission, and adds noise based on the SNR computations done in the Core- and Post-Modules.

### 3.3 Exoplanet Atmosphere Models

The NEETC incorporates synthetic spectra of a few exoplanet atmospheres that serve to demonstrate the capabilities of the instrument. We have defined a list of such reference atmospheres that cover some of the expected diversity of these worlds.

The synthetic spectra have been prepared for three cases, namely: transmission, reflected starlight and planetary thermal emission. For each exoplanet, we consider two levels of aerosol-to-gas concentrations that are broadly classified as specific to optically thin and thick haze. The thick haze configuration presents a larger aerosol-to-gas ratio, which is equivalent to a higher altitude haze layer. The transmission and reflected starlight spectra have been prepared in normalized format, i.e. referred to the unimpeded stellar brightness. The planetary thermal emission spectra have been prepared in absolute radiometric units. An internal procedure normalizes the thermal emission spectra to the observer-to-star distance and to the stellar emission spectrum. Figure 5 shows the transmission, reflection and thermal emission spectra for exoplanet GJ1214b.

The spectra are produced with well-tested routines (see [10]). Specific details on the routines, the atmospheric configurations and the list of available exoplanet atmospheres will be presented elsewhere.

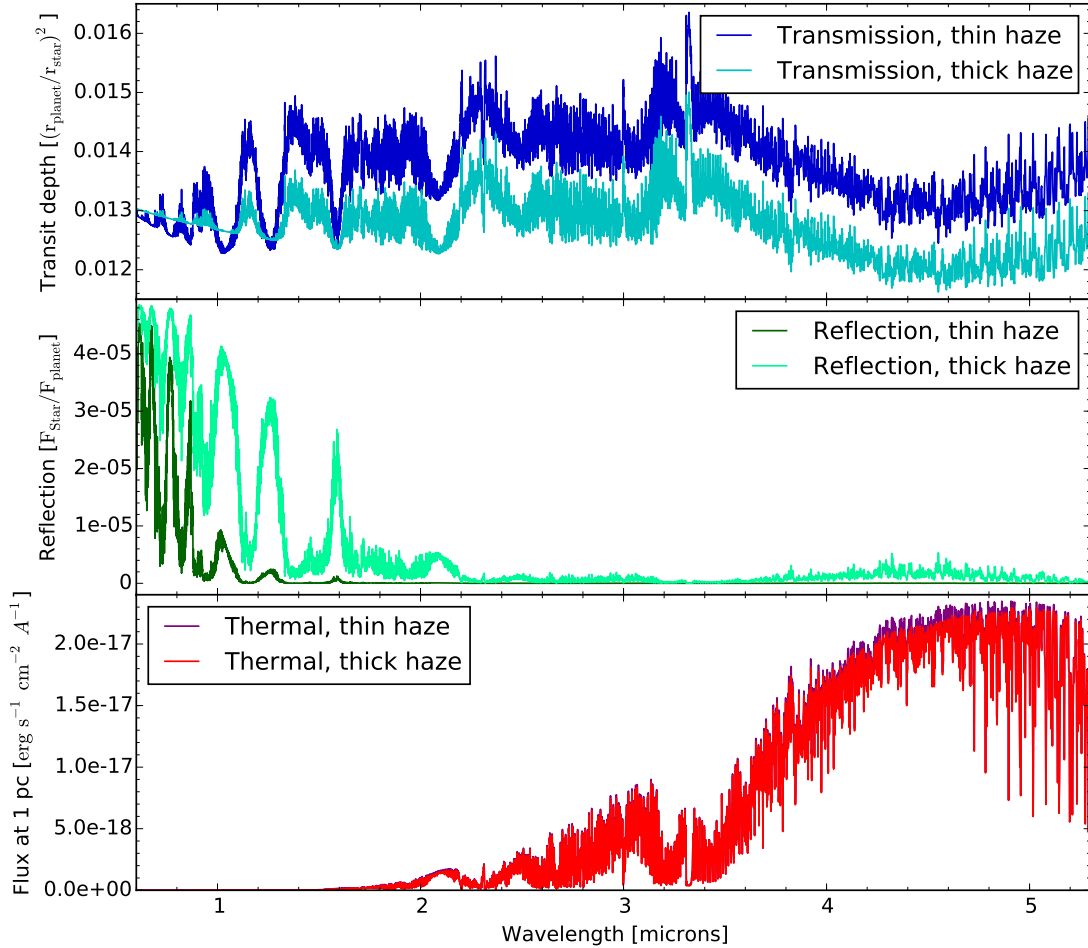


Figure 5. Synthetic planetary spectra for the warm super-Earth GJ1214b, as input to the NEETC with  $R=4000$ , for optically thin and thick haze. The transit depth and reflection of starlight are both given as the contrast to the host star. The thermal emission spectrum is the flux received at a distance of 1 pc. An internal procedure normalizes the thermal emission to the observer-to-star distance and to the stellar emission spectrum.

#### 4. EXAMPLE - TRANSIT AND OCCULTATION OBSERVATIONS OF GJ1214B

As demonstration of the NEETC capabilities, we have run a series of computations for the warm super-Earth GJ1214b [11]. The SNR computations are used to compare instrument configurations and subsequently one instrument setup is selected to generate a simulated NIRSPEC observation of the planetary spectra. Host star parameters are adopted from [12] and used to find a suitable PHOENIX template spectrum ([13], [14]) for the SNR calculations.

##### 4.1 Comparison of Instrument Configurations Based on SNR

The transit duration for GJ1214b is 52 min. The SNR for a single transit for a host star with  $T_{\text{eff}} = 3000$  K,  $\log(g) = 5.0$  (cgs units) and J-band magnitude 9.750 is calculated assuming that 52 min are spent on baseline observations before and after the transit, resulting in a total exposure time of 2hr 36min per transit. This

includes the time lost resetting the detector before every integration. Figure 6 shows the SNR for the low resolution PRISM/CLEAR configuration, using 1, 2 or 3 groups per integration ( $ng$ ). Note that a sensitivity of better than 100 ppm around 1-2  $\mu\text{m}$  is easily obtained in just one transit for a J-band magnitude 9.75 spectral type M dwarf.

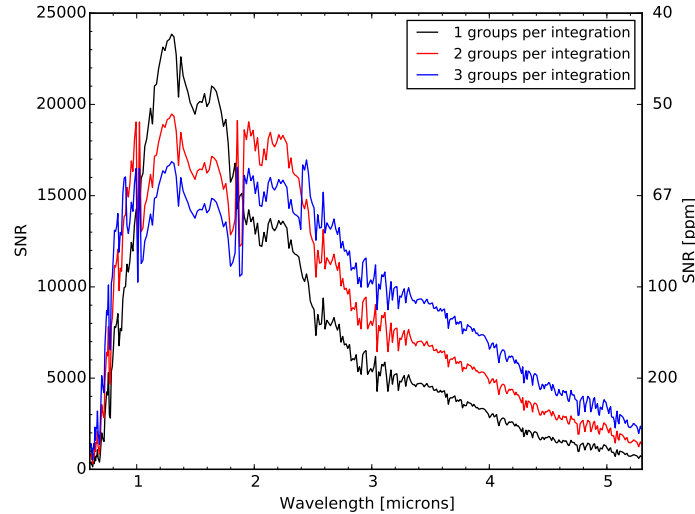


Figure 6. SNR of a NIRSPEC observation of GJ1214 with the CLEAR/PRISM configuration for one transit. Twice the transit duration is spent on baseline observations, resulting in total exposure time  $3 \times 52$  min. The NEETC has been run for a PHOENIX template spectrum with  $T_{\text{eff}} = 3000$  K,  $\log(g) = 5.0$  (cgs units) and J-band magnitude 9.750. The three curves represent the SNR for  $ng = 1, 2$  and  $3$ . SNR does not simply scale with  $ng$  due to changes in the detector duty cycle.

When moving from 1 to 2 groups per integration the SNR around 1-2  $\mu\text{m}$  goes down, as this part of the spectrum saturates after the first group. For wavelengths larger than 2  $\mu\text{m}$  the SNR goes up, as the duty cycle in this part of the spectrum goes up when using 2 instead of 1 group per integration. In other words, the efficiency goes from 50% to 66%, which increases the amount of photons collected during the complete transit. The SNR for 3 groups per integration shows further improvements for the longer wavelengths as the efficiency is increased to 75% longward of 2.4  $\mu\text{m}$ .

Which SNR-curve is the best strongly depends on the specific science case. The NEETC will provide a visual tool for the user to compare and evaluate readout setups. From Fig. 3 it is clear that GJ1214 is close to the saturation limit for the CLEAR/PRISM configuration, therefore tweaking  $ng$  has a significant effect. For the medium and high resolution configurations however, GJ1214 does not saturate for the first four groups and changes in duty cycle efficiency are less noticeable. In this case it is advisable to select the *optimal number of groups* per integration.

Figure 7 shows the SNR achieved for one transit of GJ1214, for all 9 instrument configurations, for the optimal number of groups per integration, along with  $ng = 3$  for CLEAR/PRISM. Left panel shows the SNR-curves for the inherent instrument resolution of the specific setup. In the right panel all the configurations have been re-binned to the same uniform dispersion ( $\Delta\lambda = 0.02 \mu\text{m}$ ). The medium and high resolution setups have very similar SNR, but with missing data points for the high resolution options due to the detector gaps. It indicates that the high resolution configurations are mainly useful when  $R > 1300$  is needed or for objects too bright for the corresponding medium resolution grating.

## 4.2 Simulated Transit and Emission Spectra

Simulations of the planetary signal obtained with NIRSPEC is done using the SNR for the CLEAR/PRISM configuration with  $ng = 3$ . This option gives the most uniform SNR throughout the wavelength range and

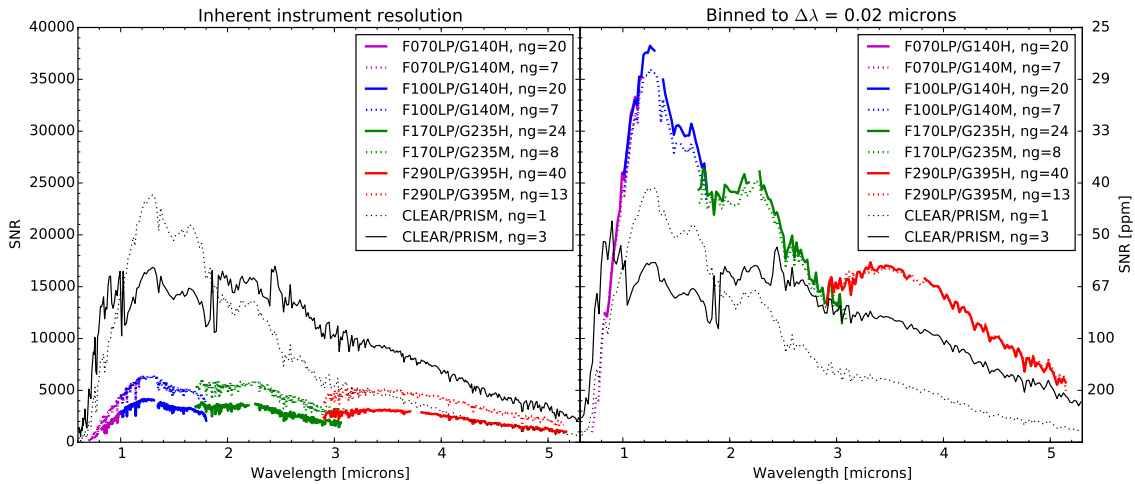


Figure 7. SNR obtainable for GJ1214 for all 9 instrument configurations for one transit (52 min). Left panel shows SNR for the inherent instrument resolution and right panel the SNR binned to a uniform dispersion of  $\Delta\lambda = 0.02 \mu\text{m}$ .

allows for a good demonstration of the science that can be done in NIRSPEC's spectral range.

For a number of transit  $n_T$ , the one sigma noise-level for the planetary signal (given as contrast to the host star) is computed as  $\sigma(\lambda) = 1/(\sqrt{n_T} \cdot SNR_T(\lambda))$  where  $SNR_T(\lambda)$  is the SNR for one transit/occultation as a function of wavelength. The transit depth for GJ1214b, based on the model described in Sec. 3.3, has been re-binned to the resolution of the CLEAR/PRISM configuration and is plotted in Fig. 8 with one sigma error bars for a single transit. The thin and thick haze cases for the planet atmosphere can clearly be distinguished in such an observation.

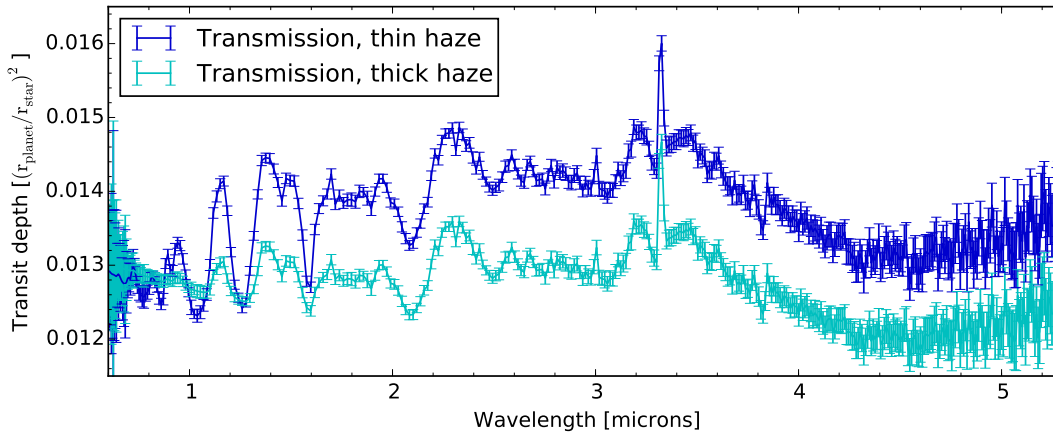


Figure 8. Simulation of a transit observation of GJ1214b with the CLEAR/PRISM configuration using 3 groups per integration. Error bars are one sigma noise based on the SNR computed for a single transit observation of the host star GJ1214.

Detection of thermal emission and reflected starlight through secondary eclipse observations will in many cases require multiple transits, as the contrast of the combined brightness compared to the host star is considerably smaller than the transit depth. The top panel of Fig. 9 shows the planet's reflection and thermal emission spectra

as a fraction of the host star flux and binned to the instrument resolution of the CLEAR/PRISM configuration. Both the low and high aerosol-to-gas concentration (thin and thick haze) spectra are presented. A distance of 12.95 pc has been adopted from [11] and is used to convert the thermal emission from the absolute values plotted in Fig. 5 to a contrast relative to the host star. The combined planet brightness, which is the observable quantity, is shown in the lower panel of Fig. 9 with the error bars ( $1\sigma$ ) corresponding to the observation of 40 occultations (assuming that the duration of the secondary eclipse is the same as the transit duration).

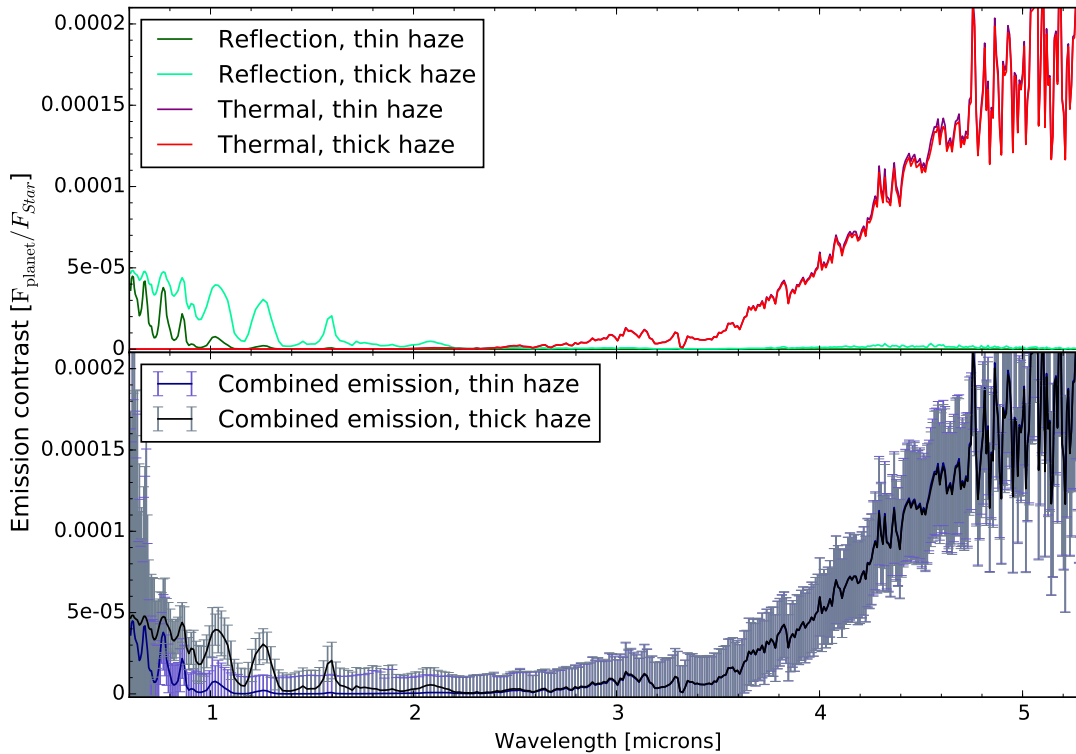


Figure 9. Simulation of 40 occultation observations of GJ1214b using CLEAR/PRISM and  $ng = 3$ . The top panel shows the synthetic reflection and thermal emission spectra as stellar contrasts. The bottom panel shows the combined emission from the planet right before and after secondary eclipse with one sigma error bars based on the SNR computed the host star.

More observations would improve the SNR, but as shown in Fig. 9, with 40 occultations the slope of the thermal emission can be constrained. GJ1214b has a visibility window of about 110 days/year with JWST. Given its short orbital period of 1.58 days and assuming a very extensive campaign, up to 70 transits could be observed within a year. In order to discriminate between the thin and thick haze models for the reflected light, the SNR can also be improved by binning the spectra in wavelength.

For the detection of reflected starlight only, it would be beneficial to use the F100LP/G140M configuration, in wavelength range 1.0 – 1.8  $\mu\text{m}$ , binned to the same resolution as that of the PRISM or lower. Judging from the the SNR curves in Fig. 7, a single transit or two could be enough to discriminate between the thin and thick haze models. Similarly, the observation can be optimized to detect thermal emission by using F290LP/G395M in the wavelength range 2.9 – 5.2  $\mu\text{m}$ . We emphasize that a single spectral configuration can be used per transit and this has to be considered when comparing the use of the PRISM to that of any grating.

## 5. FUTURE WORK AND CONCLUSION

The NEETC currently exists as a python2.7 package and has been tested by a handful of beta-users. Further development will follow to make it a more easy-to-use tool, initially for the NIRSpec instrument team and then for the general NIRSpec observer.

The example shown for GJ1214b in Sec. 4 use the stellar system as we know it, but the NEETC has been designed to produce simulated spectra for a planet similar to GJ1214b (or other planets in the library of synthetic spectra), orbiting any other given star. Users will also have the opportunity to upload planet-spectra based on their own models.

The next step in terms of input planetary signal is to develop a simple model able to generate typical planet spectra based on physical planetary parameters, such a mass, size, equilibrium temperature and albedo as well as orbital distance. This will allow us to perform a more general study of the parameter space that NIRSpec can probe. The plan is to make sure that the spectra created with this simple model can also be combined with template or user-provided spectra of the host star.

Less conservative estimates of readout noise and kTC noise along with the saturation limit of the detector will be implemented in the NEETC when more testing of the gain =  $2 e^-/ADU$  mode have been done. Non-standard subarrays, smaller than the ones listed in Tab. 1, will be supported by NIRSpec. This will allow brighter target to be observed, but also truncate the spectrum in either spatial or spectral direction. Once this truncation has been well-established, users will be able to input non-standard subarrays in the NEETC.

Choosing the best instrument and detector setup for a given observation is a trade off between SNR, spectral coverage and resolution. We foresee that SNR curves generated by the NEETC will assist the user in selecting the optimal instrument configuration for a specific science case. At the same time, the simulated planetary spectra from the NEETC will be useful to reliably prepare in-depth studies of planet atmospheres.

## REFERENCES

- [1] Kreidberg, L., Bean, J. L., Désert, J.-M., Benneke, B., Deming, D., Stevenson, K. B., Seager, S., Bert-Thompson, Z., Seifahrt, A., and Homeier, D., “Clouds in the atmosphere of the super-Earth exoplanet GJ1214b,” *Nature* **505**, 69–72 (Jan. 2014).
- [2] Gardner, J. P., Mather, J. C., Clampin, M., Doyon, R., Greenhouse, M. A., Hammel, H. B., Hutchings, J. B., Jakobsen, P., Lilly, S. J., Long, K. S., Lunine, J. I., McCaughrean, M. J., Mountain, M., Nella, J., Rieke, G. H., Rieke, M. J., Rix, H.-W., Smith, E. P., Sonneborn, G., Stiavelli, M., Stockman, H. S., Windhorst, R. A., and Wright, G. S., “The James Webb Space Telescope,” *Space Science Reviews* **123**, 485–606 (Apr. 2006).
- [3] Birkmann, S. M., Ferruit, P., Alves de Oliveira, C., Böker, T., De Marchi, G., Giardino, G., Sirianni, M., Stuhlinger, M., Jensen, P., Rumler, P., Falcolini, M., te Plate, M. B. J., Cresci, G., Dorner, B., Ehrenwinkler, R., Gnata, X., and Wettemann, T., “Status of the JWST/NIRSpec instrument,” in [*Space Telescopes and Instrumentation 2014: Optical, Infrared, and Millimeter Wave*], *Proc. SPIE* **9143**, 914308 (Aug. 2014).
- [4] Rieke, G. H., Wright, G. S., Böker, T., Bouwman, J., Colina, L., Glasse, A., Gordon, K. D., Greene, T. P., Güdel, M., Henning, T., Justtanont, K., Lagage, P.-O., Meixner, M. E., Nørgaard-Nielsen, H.-U., Ray, T. P., Ressler, M. E., van Dishoeck, E. F., and Waelkens, C., “The mid-infrared instrument for the james webb space telescope, i: Introduction,” *Publications of the Astronomical Society of the Pacific* **127**(953), 584 (2015).
- [5] Birkmann, S. M., Ferruit, P., Rawle, T., Sirianni, M., Alves de Oliveira, C., Böker, T., Giardino, G., Lützgendorf, N., Marston, A., Stuhlinger, M., te Plate, M. B. J., Jensen, P., Rumler, P., Dorner, B., Hermann, K., Mosner, P., Wright, R., and Rapp, R., “The JWST/NIRSpec instrument: update on status and performances,” in [*Space Telescopes and Instrumentation 2016: Optical, Infrared, and Millimeter Wave*], *Proc. SPIE* (2016).
- [6] Winn, J. N., “Transits and Occultations,” *ArXiv e-prints* (Sept. 2014).

- [7] Rauscher, B. J., Fox, O., Ferruit, P., Hill, R. J., Waczynski, A., Wen, Y., Xia-Serafino, W., Mott, B., Alexander, D., Brambora, C. K., Derro, R., Engler, C., Garrison, M. B., Johnson, T., Manthripragada, S. S., Marsh, J. M., Marshall, C., Martineau, R. J., Shakoorzadeh, K. B., Wilson, D., Roher, W. D., Smith, M., Cabelli, C., Garnett, J., Loose, M., Wong-Anglin, S., Zandian, M., Cheng, E., Ellis, T., Howe, B., Jurado, M., Lee, G., Nieznanski, J., Wallis, P., York, J., Regan, M. W., Hall, D. N. B., Hodapp, K. W., Böker, T., De Marchi, G., Jakobsen, P., and Strada, P., “Detectors for the James Webb Space Telescope Near-Infrared Spectrograph. I. Readout Mode, Noise Model, and Calibration Considerations,” *The Publications of the Astronomical Society of the Pacific* **119**, 768–786 (July 2007).
- [8] Ferruit, P., Birkmann, S., Böker, T., Sirianni, M., Giardino, G., de Marchi, G., Alves de Oliveira, C., and Dorner, B., “Observing transiting exoplanets with JWST/NIRSpec,” in [*Space Telescopes and Instrumentation 2014: Optical, Infrared, and Millimeter Wave*], *Proc. SPIE* **9143**, 91430A (Aug. 2014).
- [9] Barstow, J. K. and Irwin, P. G. J., “Habitable worlds with JWST: transit spectroscopy of the TRAPPIST-1 system?,” *ArXiv. Accepted as a letter in Monthly Notices of the Royal Astronomical Society* (June 2016).
- [10] García Muñoz, A., Zapatero Osorio, M. R., Barrena, R., Montañés-Rodríguez, P., Martín, E. L., and Pallé, E., “Glancing Views of the Earth: From a Lunar Eclipse to an Exoplanetary Transit,” *The Astrophysical Journal* **755**, 103 (Aug. 2012).
- [11] Charbonneau, D., Berta, Z. K., Irwin, J., Burke, C. J., Nutzman, P., Buchhave, L. A., Lovis, C., Bonfils, X., Latham, D. W., Udry, S., Murray-Clay, R. A., Holman, M. J., Falco, E. E., Winn, J. N., Queloz, D., Pepe, F., Mayor, M., Delfosse, X., and Forveille, T., “A super-Earth transiting a nearby low-mass star,” *Nature* **462**, 891–894 (Dec. 2009).
- [12] Berta, Z. K., Charbonneau, D., Bean, J., Irwin, J., Burke, C. J., Désert, J.-M., Nutzman, P., and Falco, E. E., “The GJ1214 Super-Earth System: Stellar Variability, New Transits, and a Search for Additional Planets,” *The Astrophysical Journal* **736**, 12 (July 2011).
- [13] Allard, N. F., Allard, F., Hauschildt, P. H., Kielkopf, J. F., and Machin, L., “A new model for brown dwarf spectra including accurate unified line shape theory for the Na I and K I resonance line profiles,” *Astronomy and Astrophysics* **411**, L473–L476 (Dec. 2003).
- [14] Allard, F., Homeier, D., and Freytag, B., “Model Atmospheres From Very Low Mass Stars to Brown Dwarfs,” in [*16th Cambridge Workshop on Cool Stars, Stellar Systems, and the Sun*], Johns-Krull, C., Browning, M. K., and West, A. A., eds., *Astronomical Society of the Pacific Conference Series* **448**, 91 (Dec. 2011).